Vol. 487: 135–149, 2013
doi: 10.3354/meps10368

MARINE ECOLOGY PROGRESS SERIES
Mar Ecol Prog Ser

Published July 30

Integrating field data into individual-based models of the migration of European eel larvae

Paco Melià[1,*], Marcello Schiavina[1], Marino Gatto[1], Luca Bonaventura[2], Simona Masina[3,4], Renato Casagrandi[1]

[1]Dipartimento di Elettronica e Informazione, Politecnico di Milano, Via Ponzio 34/5, 20133 Milano, Italy
[2]MOX, Dipartimento di Matematica 'F. Brioschi', Politecnico di Milano, Piazza Leonardo da Vinci 32, 20133 Milano, Italy
[3]Centro Euro-Mediterraneo sui Cambiamenti Climatici, Viale Aldo Moro 44, 40127 Bologna, Italy
[4]Istituto Nazionale di Geofisica e Vulcanologia, Viale Aldo Moro 44, 40127 Bologna, Italy

ABSTRACT: Lagrangian simulations based on coupled physical-biological models can help determine the mechanisms that affect fish recruitment, but only if the key biological and environmental drivers are accurately described. However, it is difficult to obtain experimental measurements for some vital traits, such as mortality and/or movement patterns. The different hypotheses about these traits can be contrasted by comparing simulation outputs with experimental data that can be collected in the field, such as body size distribution at selected transects. We used this approach to study the oceanic migration of European eel larvae. Despite considerable research effort (involving both field surveys and simulation studies), it is still uncertain whether this migration is a purely passive process or the result of the interaction between transport by currents and an active larval movement. Based on present knowledge of eel larvae and predictions of metabolic ecology, we developed a parameterized model that provided a simple, yet biologically reasonable description of the species' key life history traits (body growth, mortality and movement). We contrasted different model settings and identified the most plausible migration scenario by comparing simulation results against experimental data. The best-performing scenario was not purely passive but included an active larval propulsion proportional to body size. The corresponding migration duration was about 3 yr. Our modelling study succeeded in assimilating experimental data within a conceptual framework that is consistent with that sketched out, almost a century ago, by Danish biologist Johannes Schmidt.

KEY WORDS: *Anguilla anguilla* · Lagrangian simulations · Larval dispersal · Physical-biological coupling · Movement ecology · Life history traits · Data assimilation

INTRODUCTION

Investigating the mechanisms that determine the variability of fish recruitment is crucial to understand the response of fish populations to anthropogenic pressures on marine ecosystems (Gallego et al. 2007, Miller 2007, Halpern et al. 2008, Cowen & Sponaugle 2009). This is especially true for catadromous eels (genus *Anguilla*), which are characterized by a complex life cycle encompassing 2 trans-oceanic migrations. In particular, the European eel *Anguilla anguilla* has experienced a dramatic decline in abundance over the past 3 decades, and its recruitment has decreased by about 95% from the levels recorded between 1960 and 1979 (Kettle et al. 2011). Consequently, the species has recently been listed in the IUCN Red List as Critically Endangered.

*Email: paco.melia@polimi.it

The European eel is a panmictic species that reproduces in the Sargasso Sea (Als et al. 2011, Andrello et al. 2011). From this area, eel larvae (leptocephali) migrate towards Europe and North Africa. After metamorphosing into glass eels, they recruit to continental waters, where they live during their growing phase (yellow eel). After reaching sexual maturation size, adult eels undergo a second metamorphosis into silver eels and migrate back to the spawning area, where they die after reproduction (Tesch 2003). A number of factors, including changes in the oceanic environment, might have negatively affected the survival and reproductive success of *Anguilla anguilla* (Kettle et al. 2011). Sustainable management strategies for this species should therefore take into account the whole scope of its peculiar life cycle, encompassing both the continental and oceanic environments (Bevacqua et al. 2009). Studying how the ocean circulation affects recruitment patterns is critical to (1) fill one of the main knowledge gaps about eel life history and (2) assess the actual role of oceanic conditions in the eel decline (Bonhommeau et al. 2008).

Individual-based coupled physical-biological models provide a useful tool to investigate fish recruitment and contrast different hypotheses by simulation (Miller 2007). The oceanic migration of eel leptocephali has received considerable attention in the past century but, despite considerable progress towards an understanding of the biology (including physiology, ecology and behaviour) of eel larvae, many fundamental questions about their journey still remain unanswered (Righton et al. 2012). There were some early attempts to estimate the duration of American and European eel migration on the basis of oceanic surface current data (Harden Jones 1968, Power & McCleave 1983), but Kettle & Haines (2006) were the first to use an ocean circulation model to simulate the migration of European eel larvae as a passive drift of particles. Bonhommeau et al. (2009a,b) then integrated biological features, namely diel vertical migration and mortality of leptocephali, within a physical circulation model. Although recent modelling studies are a clear improvement on earlier ones, many other important biological features of the travelling particles still need to be incorporated to make simulations more realistic.

An accurate description of the major biological processes and their dependence on exogenous (such as temperature or salinity) and endogenous (such as body size or developmental stage) factors is fundamental to develop reliable models (Gallego et al. 2007), as inappropriate settings may strongly affect model predictions (Fiksen et al. 2007, Bonhommeau et al. 2010). The calibration and validation of the proposed model against experimental data is recognised as an equally important point (Hannah 2007). Nevertheless, even though field data were gathered during several oceanic surveys conducted in the past century, and were thus available to previous researchers, none of the modelling attempts performed to date has quantitatively assessed the performance of candidate models against empirical evidence.

Here we assessed the performance of different simulation scenarios in reproducing the body size distribution of European eel larvae collected at 2 reference transects during the early 1980s by McCleave & Kleckner (1987) and a collection of historical data from the Iberian Basin (McCleave et al. 1998). To this end, we used an individual-based coupled physical-biological model incorporating simple, yet biologically reasonable descriptions of body growth, mortality and movement. Our aim was to contrast different hypotheses about the development and action of key vital traits by comparing simulation outputs against experimental data.

MATERIALS AND METHODS

Ocean model

We simulated the journey of European eel leptocephali as particles in the Atlantic Ocean by using the global ocean re-analysis developed by Masina et al. (2004). Monthly mean current velocity, water temperature and salinity were obtained by data assimilation via a variational optimal interpolation scheme applied to an eddy-permitting version of the Modular Ocean Model, which covers a near-global domain (78° S to 78° N) between 1958 and 2000. Model resolution is constant in longitude and equal to 1/2°, while it varies in latitude from 1/3° between 10° S and 10° N to 1/2° at the northern boundary of the domain. Note that, although eddy-resolving, higher-resolution (1/10° or finer) ocean circulation models are available, their use is limited to hindcast experiments (i.e. to generating circulation fields by forcing the ocean with historical atmospheric reanalyses, without assimilation of oceanic data) or to short-term forecasting applications. In contrast, the model used in this study is the result of a global ocean re-analysis, obtained by constraining the ocean circulation model through the assimilation of historical ocean observations (see Masina et al. 2004 for a detailed description of the assimilation proce-

dure and the relevant results). Using assimilated models can greatly improve the realism of coupled physical-biological models (Blanke et al. 2012). They provide a more realistic reproduction of the 3-dimensional thermal and dynamic state of the ocean within the considered region, and they also improve the description of the temporal variability of the upper ocean at interannual and decadal time scales. Among assimilated models, the re-analysis used in this work is one of the best products currently available, as it has gone through an extensive validation procedure. At present, the production of global ocean reanalyses at 1/4° horizontal resolution is under way, and some products at that resolution already exist, but they do not cover the period (early 1980s) for which field data on eel leptocephali are available.

Lagrangian simulation design

In each simulation, a total of 1 000 000 Lagrangian particles per year, each particle representing a single larva, were released over a 3 yr period (1982 to 1984) and tracked for the subsequent 4 yr. This time frame was chosen to allow the simulations to be compared with experimental data gathered in that same period (see 'Experimental data for comparison with simulation outputs'). Releases were performed daily within a time window encompassing the most accredited spawning season (March to May; Schmidt 1923, McCleave & Kleckner 1987, McCleave 2008). More precisely, the probability distribution of hatchings over time was assumed to be Gaussian (with mean = 1 April and SD = 20 d). The initial geographic position of larvae was randomly drawn from a trivariate Gaussian distribution centred within the polygon identified by McCleave et al. (1987) and manually tuned to match available knowledge (Schoth & Tesch 1982, McCleave & Kleckner 1987 and references therein) about the distribution of leptocephali <10 mm in length (latitude: 26.5 ± 1.2° N; longitude: 62 ± 4° W; depth: 175 ± 35 m). The drift velocity of each particle was determined through linear interpolation of mean velocity fields in space and time. Trajectories were calculated using an explicit Euler method with a 3 h time step. The arrival line (where successful larvae were counted) was set to the 15° W meridian, further east than in previous studies (Kettle & Haines 2006, Bonhommeau et al. 2009a,b). This allowed us to extend Lagrangian simulations to the easternmost longitude at which circulation fields are not affected by the continental slope.

Biological features

Body growth

Body size is a major driver of nearly all biological rates and times (Peters 1983, Brown et al. 2004), and it plays a role in regulating vital traits of the European eel (e.g. sex differentiation, Melià et al. 2006b; sexual maturation, Bevacqua et al. 2006; natural mortality, Bevacqua et al. 2011). Therefore, it is important to identify a realistic body growth model to obtain reliable estimates of vital traits affecting migration success, such as mortality and movement (in both the horizontal and vertical direction). Schmidt (1923) proposed a body growth curve for *Anguilla anguilla* from average body length data for different months based on samples collected across the Atlantic Ocean between 1905 and 1921. His data were split into putative age groups spanning ~2 yr from egg hatching in the Sargasso Sea to the recruitment of full-grown leptocephali to European coasts. As only the body size of larvae was known and not their age, Schmidt's curve was based on an arbitrary attribution of each sampled eel to an age group. For this reason, Schmidt's arrangement of data was questioned by Boëtius & Harding (1985a), who claimed that data from I-group leptocephali (between 40 and 50 mm long), which they called 'tramps', cannot be used to assess body growth because larvae of that group can be found over most of the northern Atlantic at any time of the year. Therefore, they put forth the idea that leptocephali may begin metamorphosing into glass eels within only 12 to 15 mo. This hypothesis was also supported by the analysis of daily growth increments in otoliths (Castonguay 1987, Lecomte-Finiger 1992, Wang & Tzeng 2000), but strongly criticized by McCleave (2008) and Zenimoto et al. (2011). As no irrefutable evidence has been found in favour of either hypothesis, we considered a set of 4 candidate growth curves consistent with both interpretations (Fig. 1). We fitted Schmidt's (1923) data (from his Fig. 8) under the hypothesis of a 2.5 yr long larval phase with a power function (PF), by visual inspection of the data, and with a von Bertalanffy (VB) curve, a common choice for modelling body growth in fish. These 2 body growth models are indicated as PF-slow and VB-slow in Fig. 1a. To contrast Schmidt's interpretation of data with that by Boëtius & Harding (1985a), we also fitted both functions against a rearranged dataset from which I-group leptocephali (grey circles in Fig. 1a) were removed. Under the hypothesis that the larval phase lasts only 1.5 yr, we assigned the largest larvae collected between February

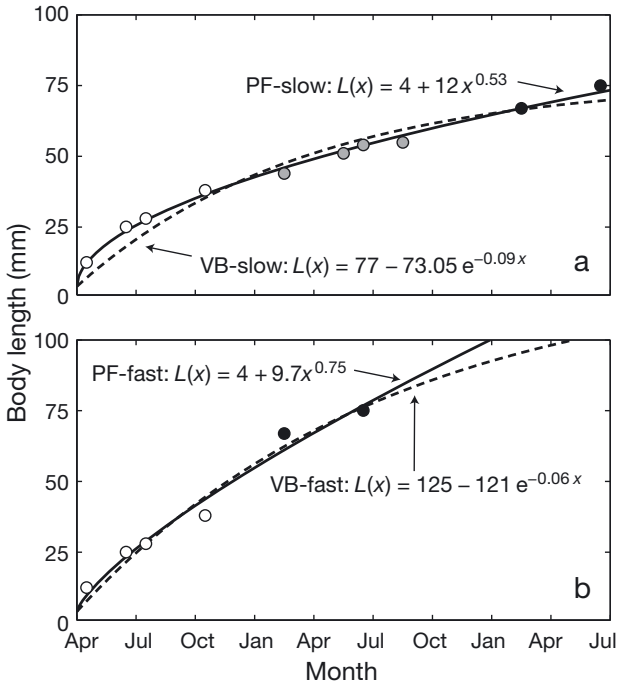

Fig. 1. Body growth sub-models for European eel leptocephali (see Table 1). (a) Power function (PF-slow) and von Bertalanffy (VB-slow) curves fitted to the original body length data compiled by Schmidt (1923; his Fig. 8). Circles with different shadings indicate 3 putative age groups (0, 1 and 2 yr). (b) Power function (PF-fast) and von Bertalanffy (VB-fast) curves fitted to Schmidt's data filtered according to the reanalysis by Boëtius & Harding (1985a), i.e. removing I-group leptocephali (grey circles in a) and subtracting 1 yr from the age of the largest leptocephali (black circles in a)

and June (black circles in Fig. 1a) to the second age class (and not to the third, as done by Schmidt). These 2 models are graphically represented in Fig. 1b and indicated as PF-fast and VB-fast. In conclusion, 4 body growth models, differing with respect to the functional form and the supposed duration of the larval phase, were fitted to Schmidt's (1923) original data or to a subset of it (sensu Boëtius & Harding 1985a). All curves showed good fitting performances (R^2 between 0.95 and 0.99).

To account for inter-individual body growth variation (typical of fish species characterized by high body growth plasticity, such as *Anguilla anguilla*; Tesch 2003), we used an individual-based body growth model. In particular, we used an assignment-at-birth scheme (Kirkpatrick 1984) similar to that used to describe body growth in the continental phase of European and New Zealand eels (De Leo & Gatto 1995, Hoyle & Jellyman 2002). The realized body length $l(x)$ of an individual at age x was expressed as the product between the expected length predicted by the relevant deterministic model $L(x)$ and a random factor assigned at hatching (g). In accordance with data from glass eels recruited in the Mediterranean Sea (Melià et al. 2006a), we assumed that the natural logarithm of g follows a Gaussian distribution with mean = 0 and standard deviation $\sigma = 0.056$.

Mortality

So far, the only assessment of natural mortality during the oceanic migration of European eel larvae is that obtained by Bonhommeau et al. (2009b). In the absence of any experimental data on larval survival, however, their estimate relies on model simulations driven under the hypothesis that the global eel stock was stationary during the period considered in the study (1960 to 2004); however, during this time window, the European eel stock underwent its dramatic decline (Kettle et al. 2011). To avoid this stringent hypothesis, we followed the approach of Bevacqua et al. (2011), which relied on the metabolic theory of ecology (Brown et al. 2004). Bevacqua et al. (2011) linked eel mortality μ in the continental phase to water temperature T (through a Boltzmann-Arrhenius factor) and body mass M (through an allometric function):

$$\mu = a \times \exp(-E/kT) \times M^b \quad (1)$$

where a is a proportionality coefficient, E is the activation energy, k is the Boltzmann constant (= 8.62×10^{-5} × eV K^{-1}) and b is an allometric exponent. While scaling parameters such as b and E can be supposed to hold over the whole life cycle of the species, a is affected by factors that cannot be extrapolated from the continental to the larval oceanic life stage. In the continental phase, the natural logarithm of a is reported to range between 48.5 and 50.8 depending on eel gender and stock density (Bevacqua et al. 2011). For the oceanic phase, after performing some explorative simulations to identify a plausible range of survival probabilities, we tested a set of tentative values for a ($\ln[a]$ between 46 and 48) and assessed the sensitivity of the results to this parameter. In fact, for values of $\ln(a)$ greater than 48 (such as those obtained by Bevacqua et al. 2011) migration success was null (no larvae, out of the 3 000 000 released, survived the migration), while $\ln(a) = 46$ was the minimum value compatible with computational intensity.

Estimating mortality rate through the model described above requires knowledge of the body mass of larvae, not just the body length. Unfortunately, no data on the body mass of European eel larvae are available in the literature, thus hindering the estima-

tion of a specific morphometric relationship. For this reason, we linked body mass M (in g) with body length L (in mm) by using the allometric function proposed by Melià et al. (2006a) for undifferentiated yellow eels, i.e. $M = 2.24 \times 10^{-7} \times L^{3.37}$. Although the validity of extrapolating a morphometric relationship from one life history stage to a very different one may be questionable (due to the different body mass composition and body shape between the 2 stages), body mass predicted by this function seems reasonable within the body length range of European eel leptocephali, and a comparison with published data on leptocephali of other eel species suggests that our margin for error is acceptable (Fig. S1 in Supplement 1 at www.int-res.com/articles/suppl/m487p135_supp1.pdf).

Movement

Information about the interplay between navigation capacity and motion ability in generating movement paths (sensu Nathan et al. 2008) is available only for a small number of species (Holyoak et al. 2008). As for the swimming ability of adult European eels, we know that they can cover the distance between Europe and the Sargasso Sea with a remarkable efficiency and at low energy costs (van Ginneken et al. 2005). Little is known about the swimming performances of eel larvae, and nothing on the species-specific movement of *Anguilla anguilla* larvae. However, Wuenschel & Able (2008) assessed the swimming speed of *A. rostrata* glass eels and *Conger oceanicus* metamorphosing leptocephali, showing that the sustained swimming speed of both species ranges between 5.8 and 9.3 cm s^{-1}, corresponding to ca. 0.9 to 1.1 body lengths per second (BL s^{-1}). In our simulations, we have compared the results derived under the hypothesis of a purely passive drift with those obtained with increasing levels of larval propulsion (locomotion). We assumed swimming speed to be proportional to body length (Peters 1983) within a plausible speed range from 0 (passive drift) to 4 BL s^{-1}. Of course, if leptocephali swam continuously at their maximum speed, they would probably not be able to feed properly. For this reason, the swimming speeds considered in our scenario should be considered as average values.

In contrast with Bonhommeau et al. (2009a,b), who hypothesized that eel larvae can regulate their depth to match the maximum current velocity, we did not consider a vertical rheotaxis. In fact, although larvae may perceive local gradients, it is quite unlikely that they can react to current profiles over the whole water column. However, we assumed that leptocephali have a horizontally rheotactic behaviour. The ability of fishes to use their mechanosensory lateral line system to mediate rheotaxis (Montgomery et al. 1997) has been observed in several lab studies (e.g. Olszewski et al. 2012), and the results of a recent study on green sturgeons (Kelly & Klimley 2012) suggest that fish can orient their swimming with respect to the current direction even in the open sea. Therefore, active swimming simulations were performed by adding a size-specific individual propulsion to the modulus of the drift velocity.

Besides horizontal movement, eel larvae also exhibit a diel vertical migration (Castonguay & McCleave 1987), possibly driven by a negative phototaxis and/or an entrained circadian rhythm (Yamada et al. 2009) most likely determined by their antipredator behaviour. Previous Lagrangian simulations by Bonhommeau et al. (2009a,b) and Zenimoto et al. (2011) approximated this behaviour by letting eel larvae switch between 2 fixed depths (50 m at night and 300 m at day). However, younger larvae collected during the day between the Sargasso Sea and the Gulf Stream, i.e. at the beginning of their migration, were found at a shallower depth than older eel larvae caught on the continental shelf west of France and the British Isles, i.e. at the end of the migration (Tesch 1980, Castonguay & McCleave 1987). In the absence of any information about the vertical distribution of leptocephali during the rest of their journey across the ocean, we considered it reasonable to assume that daytime depth increases with body length.

Although previous studies did not consider interindividual variation in the vertical distribution of leptocephali, the analysis of oceanic circulation fields reveals that changes in current direction and intensity may take place also within relatively small depth ranges. As these changes may have a strong influence on the migration paths of different individuals, we incorporated an individual-based stochastic component into diel vertical migration. At night (from 21:00 to 6:00 h), the vertical position of each larva was drawn randomly at every time step from a Gaussian distribution, with parameters (mean ± SD = 60 ± 25 m) kept constant during the journey. In contrast, during the day (from 9:00 to 18:00 h) larvae were randomly distributed around a mean depth increasing linearly with body length from 73.5 m at L = 5 mm to 470 m at L = 80 mm, with a constant SD of 25 m. To account for the time required to shift from one depth to the other and vice versa, we considered 2 intermediate steps (from 6:00 to 9:00 h and

from 18:00 h to 21:00) in which the vertical position of the larvae was randomly distributed around the average of night and day mean depths.

Experimental data for comparison with simulation outputs

To provide a comparison with the earliest and latest phases of the migration, we chose datasets from both the western and eastern side of the ocean. Unfortunately, we could not find a suitable dataset relevant to the central part of the eel migration. For the west side, we used data from 2 cruises conducted in summer (July/August) and autumn (September/October) 1984 between the Sargasso Sea and the Florida Current (McCleave & Kleckner 1987, McCleave et al. 1998). The 2 samples are referred to as Florida/Summer (FS) and Florida/Autumn (FA) hereafter. For the east side, we used the data reported in McCleave et al. (1998), which summarize the collection of historical data compiled by Boëtius & Harding (1985b) and data collected in summer 1984 in the Iberian Basin (IB) (Bast & Strehlow 1990). These data consist of mean body length and standard deviation for 3° latitude by 4° longitude cells spanning between 32° to 65° N and between 3° and 35° W. To derive a sample to be compared with our simulation results, we proceeded as follows. For each cell, we drew a congruous (i.e. proportional to the abundance of the experimental sample) random sample from a normal distribution with the same mean and SD, thus obtaining a statistically equivalent length distribution. After repeating the draw for each cell adjacent to the 15° W meridian, we merged the synthetic distributions of all cells to derive a synthetic body length distribution along our arrival line. Reference body length distributions at the 3 transects are shown in Fig. 2.

Identifying the best simulation scenarios

Tracking Lagrangian particles over the spatial and temporal domain covered by our simulations is computationally intensive, and a rigorous calibration of all 3 sub-models would not be feasible. Hence, we identified a set of plausible values for the most critical parameters of our 3 sub-models (Table 1) and assessed the realism of different simulation scenarios by comparing the results of the relevant simulations with experimental data. The combination of different parameter settings for the 3 sub-models resulted in 4 × 5 × 5 = 100 simulation scenarios.

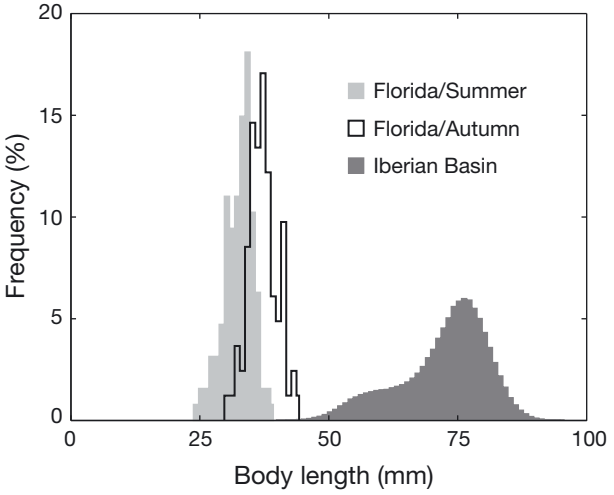

Fig. 2. Body length distribution of European eel leptocephali at 3 reference transects: Florida/Summer and Florida/Autumn (data from Fig. 4C of McCleave et al. 1998), and Iberian Basin (data from Fig. 2 of McCleave et al. 1998). Data derived as described in 'Materials and methods: Experimental data for comparison with simulation outputs'

Table 1. Summary of the settings for the different simulation scenarios. A scenario is defined by a combination of 3 settings, one for each sub-model. In the text and figures, scenarios are identified through a short description of the relevant sub-models: for instance, 'PF-slow growth with medium mortality and moderate speed' indicates a model including a power function describing body growth, fitted on Schmidt's (1923) original data, an intermediate mortality rate ($\ln[a]$ = 47.0 in Eq. 1) and an active locomotion at a swimming speed of 1 body length (BL) s^{-1}

Body growth sub-model (see Fig. 1)	
PF-slow	Power function fitted to Schmidt's (1923) original data
VB-slow	Von Bertalanffy curve fitted to the same data as PF-slow
PF-fast	Power function fitted to Schmidt's (1923) data by removing I-group leptocephali as suggested by Boëtius & Harding (1985a)
VB-fast	Von Bertalanffy curve fitted to the same data as PF-fast
Mortality sub-model	
Very low mortality	$\ln(a) = 46.0$
Low mortality	$\ln(a) = 46.5$
Medium mortality	$\ln(a) = 47.0$
High mortality	$\ln(a) = 47.5$
Very high mortality	$\ln(a) = 48.0$
Locomotion sub-model	
Passive drift	0 BL s^{-1}
Low speed	0.5 BL s^{-1}
Moderate speed	1 BL s^{-1}
High speed	2 BL s^{-1}
Very high speed	4 BL s^{-1}

The performance of each scenario was evaluated, taking into account the ability of the model to reproduce observed body size patterns of leptocephali. First, we intercepted Lagrangian particles along the reference transects described in the previous section over the relevant time frame (i.e. during the period in which the transects were actually sampled in the field). Second, we assessed the predictive ability of each scenario along each transect through 2 discrepancy indicators: the absolute percent error on the median, e_{median}, and the absolute percent error on the interquartile range, e_{iqr}, defined as:

$$e_{median} = |median(L) - median(\hat{L})|/median(L) \quad (2)$$

$$e_{iqr} = |iqr(L) - iqr(\hat{L})|/iqr(L) \quad (3)$$

where median(L) and median($\hat{L}$) are observed and simulated median body lengths, respectively, and iqr(L) and iqr($\hat{L}$) the observed and simulated interquartile ranges of body length, respectively. After calculating e_{median} and e_{iqr} for each of the 3 transects, we calculated the overall discrepancy (d) of each scenario with respect to the median and interquartile range as the following Euclidean norms (subscripts FS, FA, IB indicate the relevant reference transects):

$$d_{median} = \sqrt{e^2_{median,FS} + e^2_{median,FA} + e^2_{median,IB}} \quad (4)$$

$$d_{iqr} = \sqrt{e^2_{iqr,FS} + e^2_{iqr,FA} + e^2_{iqr,IB}} \quad (5)$$

Therefore, the 2 indicators d_{median} and d_{iqr} summarize the discrepancy between observations and simulations with respect to (1) central tendency, (2) inter-individual variability and (3) spatial variability (by averaging discrepancy across the 3 transects) of body size distribution. Finally, to identify the best scenario we looked, from a multi-criteria perspective, for the best trade-off between minimizing the 2 indicators d_{median} and d_{iqr}.

RESULTS

Lagrangian simulations

For each simulation scenario, we calculated the statistics of interest for migration duration, migration success and latitudinal distribution across the 15° W meridian, assumed to be the arrival line for eel larvae (for a full summary see Supplement 2 at www.int-res.com/articles/suppl/m487p135_supp2.xls). We also derived the body length structure at the 3 reference transects. Depending on the scenario (see Table 1), the average duration migration from the Sargasso Sea to the 15° W meridian was between 21 mo (PF-fast growth, very high mortality and very high speed) and 41 mo (VB-slow growth, all mortality rates, passive drift). Migration success ranged between 0.001% (very high mortality) and 7% (very low mortality) for active locomotion scenarios, while in passive drift scenarios at very high mortality no eel larvae reached the arrival line. Mean latitude of arrivals varied between 38–39° N (very high speed) and 52–54° N (passive drift). Median body length ranged between 24 mm (VB-slow growth, very high mortality and moderate speed) and 36 mm (PF/VB-fast growth and very high speed) at the FS transect, between 35 mm (VB-slow growth) and 46 mm (VB-fast growth, very high mortality and low speed) at the FA transect and between 68 mm (PF-slow growth, moderate to high speed) and >100 mm (PF-fast growth) at the IB transect (15° W).

Comparison with experimental data

Fig. 3 shows the performance of the 100 scenarios as synthesized by the 2 indicators d_{median} and d_{iqr}. Note that lower values of d_{median} and d_{iqr} indicate better performances: therefore, the symbols in the left-bottom corner of Fig. 3a represent the best-performing scenarios. Slow body growth curves (both PF and VB) perform better (in terms of median body size at the reference transects) than those derived by removing I-group leptocephali, as suggested by Boëtius & Harding (fast body growth). Also, the power function model (PF-slow growth) matches observed inter-individual body size variation better than the corresponding von Bertalanffy curve (VB-slow growth), and the relevant scenarios are therefore characterized by a lower d_{iqr}. As for locomotion, scenarios considering active swimming at low to high speed perform better than those considering a passive drift or active swimming at high speed (Fig. 3b). The value attributed to mortality rate does not greatly influence the realized body size distribution at the selected transects, but it does affect migration success and duration (see 'Discussion: Mortality').

All best-performing simulation scenarios share the same body growth curve (PF-slow growth). The scenario that best reproduces median body size at the reference transects, i.e. minimizes d_{median}, is indicated as Sc1 in Fig. 3 and has a very high mortality rate and active swimming at moderate speed (1 BL s^{-1}). On the other hand, the scenario that best matches the observed dispersion around the central

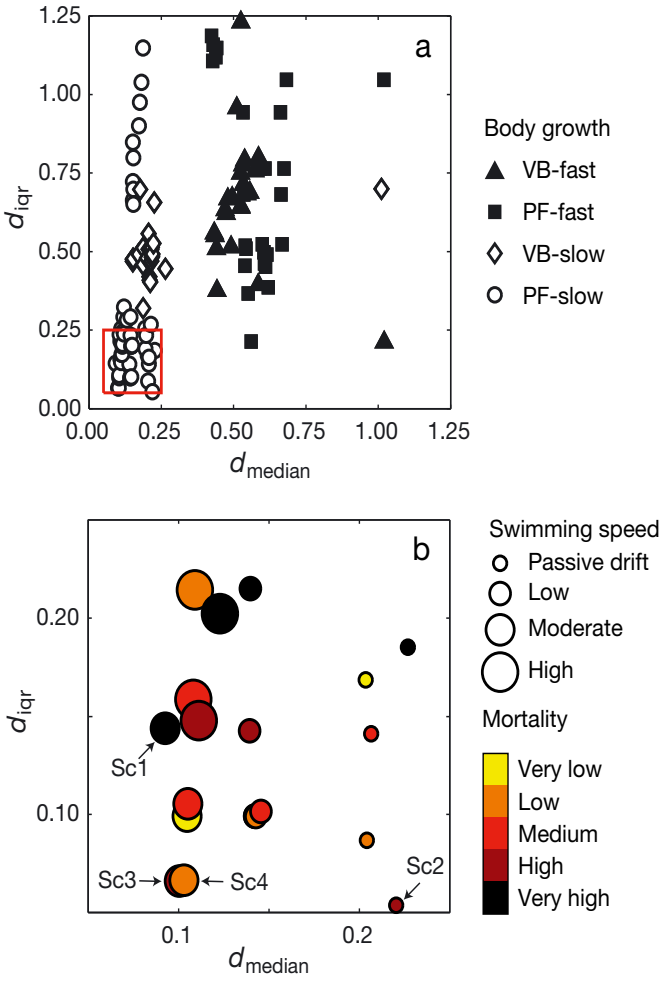

Fig. 3. Fitting performances of 100 simulation scenarios (see Table 1) reproducing the oceanic migration of European eel leptocephali. d_{median} and d_{iqr} measure the discrepancy between observed and simulated median and interquartile range of body length, respectively (see 'Materials and methods: identifying the best simulation scenarios'). Lower values of d_{median} and d_{iqr} indicate increasing performances. Scenarios (identified by symbols) are classified by (a) the settings of body growth sub-models, and (b) mortality and locomotion sub-models. Panel (b) shows only the best-performing scenarios (red box in a), all sharing the same body growth function (PF-slow growth). The specific parameter settings of the 4 best performing scenarios, indicated as Sc1, Sc2, Sc3 and Sc4 in (b), are described in 'Results: Comparison with experimental data'

tendency, i.e. minimizes d_{iqr}, is indicated as Sc2 and has a high mortality rate and passive transport. However, there are 2 scenarios (Sc3 and Sc4), both characterized by active swimming at moderate speed but slightly different mortalities (high and low), which provide a good trade-off between minimizing the performance indicators. Compared with Sc1, scenarios Sc3 and Sc4 guarantee a remarkable decrease in d_{iqr} that offsets a modest increase in d_{median}; at the same time, they guarantee a considerable decrease in d_{median} compared to Sc2, while determining an acceptable increase in d_{iqr}. As the performances of Sc3 are slightly better than those of Sc4 with respect to both indicators, we consider Sc3 as the reference scenario and analyse it in more detail.

The ecologically important characteristics of our reference scenario — characterized by Schmidt's body growth curve (PF-slow), high mortality rate and moderate swimming speed — are summarized in Figs. 4 to 6. Fig. 4 shows the simulated frequency distribution of migration duration and the latitudinal distribution of successful larvae. Migration duration has a peak at ca. 26 mo, with an average of about 30 mo from the Sargasso Sea to the arrival line. The latitudinal distribution of arrivals has a main peak in front of the Bay of Biscay (between ca. 45 and 50° N) and a secondary one off Moroccan coasts (at about 35° N). Fig. 5 compares the spatial distribution of all released larvae (Fig. 5a) with the starting location of only those successfully arriving at the 15° W meridian within 4 yr (Fig. 5b). The majority of successful larvae began their journey from a small central area within the polygon identified by McCleave et al. (1987), namely the region between 25–30° N and 50–65° W. Finally, Fig. 6 shows the simulated occurrence limits of leptocephali of different body size, which are consistent with those derived by Schmidt (1923; his Fig. 4) on the basis of field samples.

DISCUSSION

Identifying the simulation scenario that best reproduces experimental body length distributions at the different transects does not prove per se that the biological mechanisms included in the model are correct. However, it corroborates the underlying hypotheses against alternative ones that fail in assimilating experimental data within a consistent conceptual framework. In the following, we discuss the most plausible conclusions that can be drawn from our simulation study, and contrast them with current knowledge about the migration of eel leptocephali.

Body growth

A power function based on a 2.5 yr migration hypothesis (PF-slow growth) fits Schmidt's (1923) data very closely. Fig. 7 compares observed and simulated body length distributions at the 3 reference transects, as obtained by simulation under reference

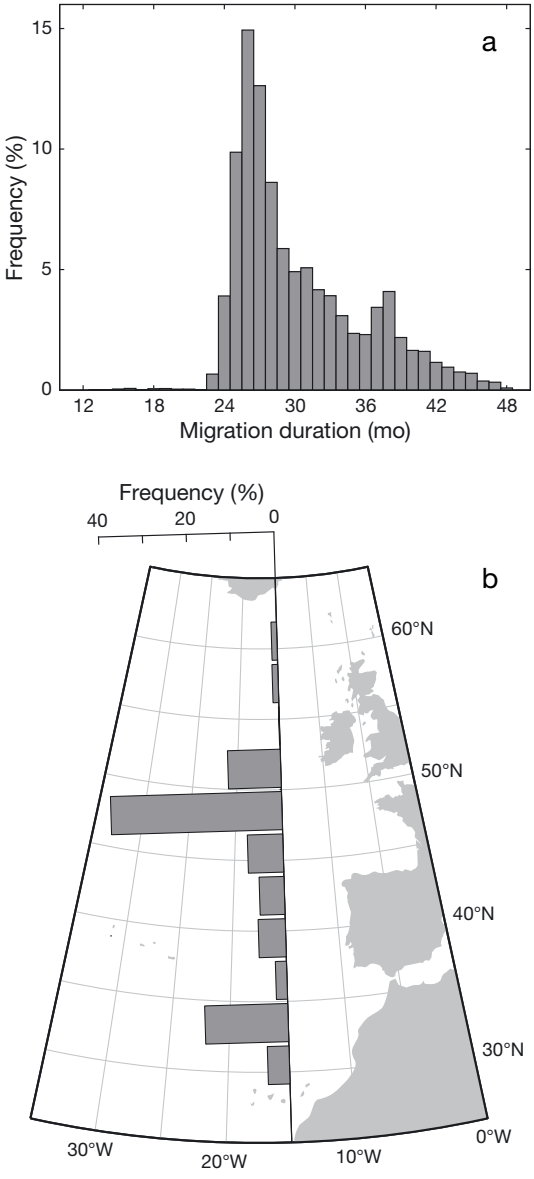

Fig. 4. Frequency distribution of (a) migration duration and (b) latitude of European eel leptocephali successfully reaching the 15° W meridian within 4 yr, as obtained by simulation under reference scenario Sc3 (see Fig. 3 and 'Results: Comparison with experimental data')

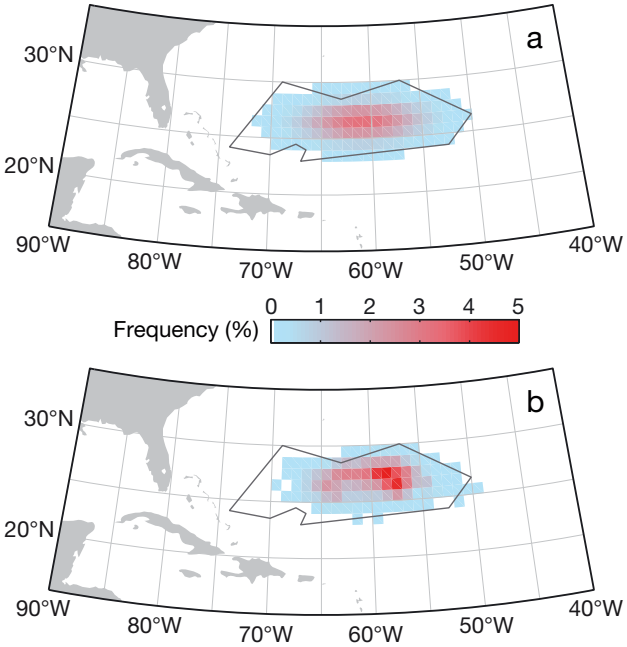

Fig. 5. Comparison between the spatial distribution of starting locations (a) for all Lagrangian particles released within the spawning region identified by McCleave et al. (1987) and (b) for the subset of particles that successfully crossed the 15° W meridian within 4 yr under reference scenario Sc3 (see 'Results: Comparison with experimental data')

scenario Sc3. The curves derived under the hypothesis of a fast growth (PF/VB-fast growth) provided a slightly better fit of the body length distribution at the FS transect compared with those derived by assuming a slower growth, consistent with Schmidt's original view. However, this hypothesis failed to reproduce the body length distribution at the FA transect. The error was even larger at the arrival line, because the shortest simulated migration duration (21 mo) was still too long to be consistent with the fast growth hypothesis (1.5 yr migration). As a consequence, estimated body lengths at the IB transect under the fast-growth hypothesis were unrealistically high (>100 mm), irrespective of the settings used for the mortality and locomotion sub-models. On the other hand, the VB-slow growth model was not able to accurately reproduce the body growth patterns observed in the earliest developmental stages, while growth rates predicted by the power function were in good accordance with available information on early larval development of other eel species. In fact, the model predicted an average body growth rate of 0.32 mm d^{-1} for the first 50 d, and 0.14 mm d^{-1} between the 50th and the 100th day of life, very close to the values reported for laboratory-grown leptocephali of *Anguilla japonica* (Tanaka et al. 2001, Tsukamoto et al. 2009). A similar growth rate (0.28 mm d^{-1}) was also reported for *A. rostrata* in the first 5 d after hatching (Oliveira & Hable 2010). Assessments of body growth rate in different eel species based on otolith microstructure analysis (e.g. Castonguay 1987, Kuroki et al. 2006, Shinoda et al. 2011) provided remarkably higher estimates, but might have been affected, as put forth by Zenimoto et al. (2011), by a reduced deposition of otolith increments at low temperatures.

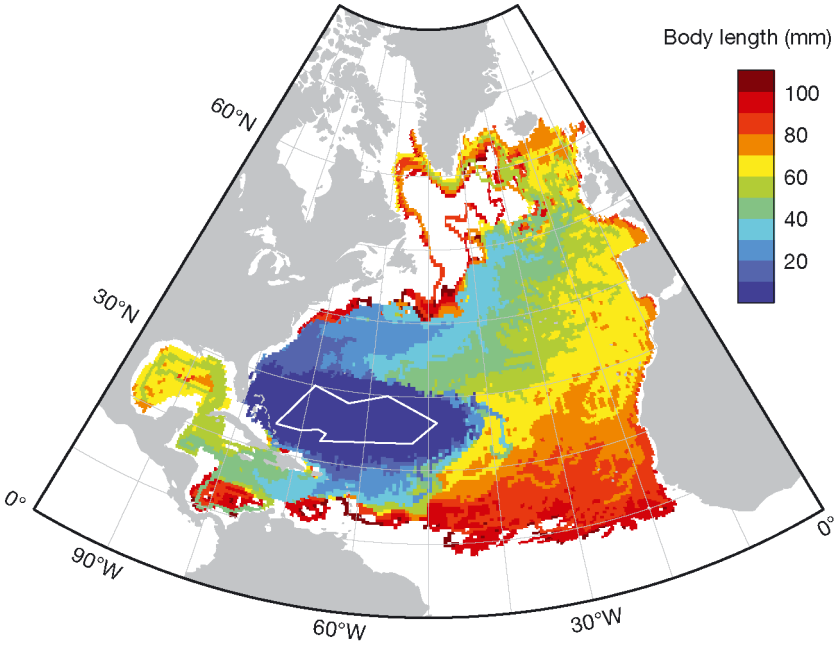

Fig. 6. Occurrence limits for European eel leptocephali of different body length, as obtained by simulation under reference scenario Sc3 (see 'Results: Comparison with experimental data'). The colour of each cell represents the maximum length of all leptocephali that passed through the cell during their migration. The spawning region identified by McCleave et al. (1987) is marked in white

Mortality

Simulated body length distributions at the reference transects were not markedly affected by the assumed mortality rate. Therefore, the simulations did not provide any evidence about a likely range for this crucial parameter. In contrast, mortality had a pronounced effect on larval survival. Under the most favourable scenarios for body growth and locomotion (PF-slow growth and moderate swimming speed), migration success varied between 0.04 and 7% depending on the setting of the mortality sub-model. This wide range (spanning 3 orders of magnitude) encompasses the estimate (0.12%) obtained by Bonhommeau et al. (2009b) under a steady-state hypothesis of the European eel population. Under the mortality setting associated with reference scenario Sc3, migration success was 0.42%. A considerable proportion (>60%) of leptocephali dies during the first month of life. Interestingly, the combined effect of the variation in body size (increasing from 4 mm at birth to ca. 75 mm at the 15° W meridian) and water temperature (decreasing from ca. 21°C in the Sargasso Sea to ca. 14°C near European shelves) determines a steep decrease of mortality rate along the journey of leptocephali, from 0.14 d^{-1} at birth to 0.00042 d^{-1} (= 0.15 yr^{-1}) at the end of the migration.

Despite the difficulty of identifying the most realistic mortality scenario in the absence of any data about larval survival, estimates of migration success can be used to derive a rough assessment of the global spawning stock. On the basis of a 'Procrustean' estimate of 2 billion glass eels recruiting each year to European coasts (Dekker 2000), assuming a 20% hatching rate and a fecundity of 1.5 million eggs per female (Bonhommeau et al.

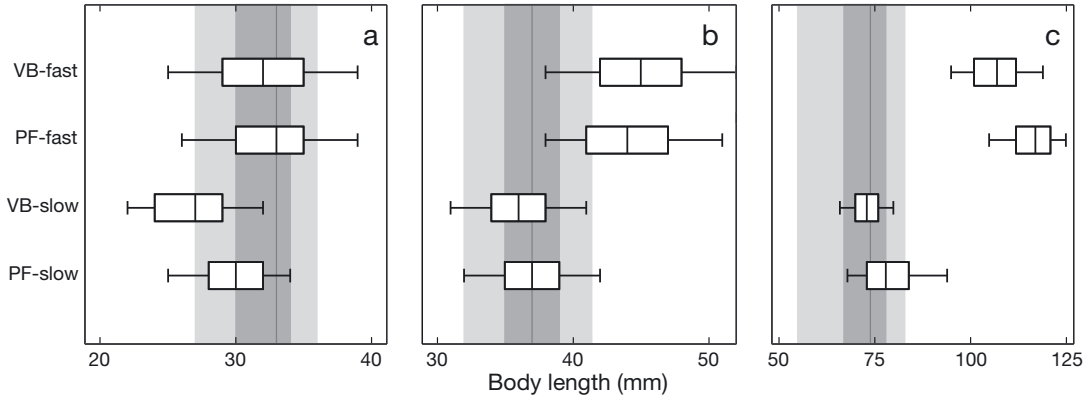

Fig. 7. Simulated body length distributions of European eel leptocephali at the 3 reference transects: (a) Florida/Summer, (b) Florida/Autumn and (c) Iberian Basin, as obtained from 4 simulations with settings (details in Table 1) for mortality (high level) and locomotion (active, moderate speed) as in reference scenario Sc3 (see 'Results: Comparison with experimental data'), but differing with respect to body growth (see Fig. 1). Boxes: interquartile range; vertical line: median; whiskers: 90% confidence intervals. Box-whisker plots are superimposed on a shaded area showing the body length distribution experimentally observed at each transect (straight line, darker shading and lighter shading indicate median, interquartile range and 90% CI, respectively)

2009b), the spawning stock would range between 91 000 and 15 million spawning females depending on the selected mortality scenario, with a 'best' estimate of 1.6 million spawners.

Movement

Whether the oceanic migration of eel larvae is a purely passive process of long duration (2 to 3 yr) or an (at least partially) active process of short duration (1 yr or less) is the subject of long-standing debate (van Ginneken & Maes 2005, McCleave 2008). Our simulations suggest that active locomotion is an important factor in determining migration duration. The best-performing scenarios were those that assumed a swimming speed of 1.0 BL s^{-1}. Some scenarios at 0.5 BL s^{-1} were also good in terms of overall performance, but they were less satisfactory in reproducing the observed length distribution at the 15° W meridian (i.e. they overestimate body length). A swimming speed between 0.5 and 1.0 BL s^{-1} is consistent with estimates reported for migrating adults of different eel species (van Ginneken & Maes 2005). Compared with a passive drift scenario, swimming at 1.0 BL s^{-1} reduces the migration duration by 18 to 21%. The introduction of active locomotion has the most remarkable consequences on migration success. In fact, swimming at 1.0 BL s^{-1} guarantees in our simulations a 6- to 12-fold increase of migration success compared with analogous scenarios based on passive migration.

Some of the observed discrepancies between the results of previous simulations and ours may arise from the different modelling approach used to describe the movement of eel larvae. To assess the consequences of different assumptions about vertical movement, we compared the results obtained with our reference simulation scenario Sc3 with those of 2 additional scenarios sharing the same settings except that the diel vertical migration was described (1) with larvae maintaining the same depth throughout the migration route, as in Kettle & Haines (2006), and (2) with larvae switching between 2 fixed depths (50 m at night and 300 m at day), as in Bonhommeau et al. (2009a,b). Results are reported in Supplement 2. While migration duration and body length distribution at the reference transects were not appreciably affected by modifying vertical movement pattern, migration success was strongly affected. Success rate was remarkably higher (1.66% instead of 0.42%) for the single-depth scenario and lower (0.18%) for the 2-depth scenario compared to the reference simulation scenario. This is in accordance with the findings of Bonhommeau et al. (2009a, 2010) and suggests that diel vertical migration might be aimed at maximizing migration success by minimizing mortality rather than minimizing migration duration.

Migration duration

The average migration duration to the 15° W meridian associated with the reference scenario is ~2.5 yr. Considering the residual distance that leptocephali must cover to reach European shelves, the longitudinal component of the oceanic velocity field across that transect and the contribution of larval propulsion, it is possible to estimate a further 1 to 2 mo to complete the migration. This means that leptocephali would reach Europe in late autumn, metamorphose into glass eels in the subsequent 1 to 2 mo (Arai et al. 2000) and recruit to continental waters after a further 2 to 3 mo (Wang & Tzeng 2000), between late winter and spring (Desaunay & Guérault 1997). This schedule fits perfectly with that sketched out, almost one century ago, by Schmidt (1923). It is also consistent with the estimated 3 yr time lag between primary production in the Sargasso Sea and glass eel recruitment to European coasts (Bonhommeau et al. 2008), and with the view that otolith microstructure analysis provides a large underestimation of migration duration, as already argued by McCleave (2008). In fact, Zenimoto et al. (2011) showed that the discrepancy between age estimates resulting from cohort analysis and those derived through otolith microstructure analysis can be ascribed to the effect of temperature on the deposition rate of otolith increments. By using their approach to simulate temperature-dependent otolith deposition, we estimated an 'apparent' age of ~19 mo, which is more similar to the estimates obtained by the most recent otolith microstructure analyses (Wang & Tzeng 2000) than to the true age of particles reaching the arrival line. In contrast, Bonhommeau et al. (2009b) estimated a mean migration duration of only 18 mo (to reach the 20° W meridian), to which they added another 3 mo for leptocephali to reach Europe and metamorphose into glass eels. This implies a migration schedule longer than that suggested by otolith microstructure analysis, but shorter than that resulting from cohort analysis and our Lagrangian simulation experiments. Besides the differences in the description of active movement, this discrepancy also results from the different spatiotemporal settings used for larval release. To assess how these settings affect our results, we ran 2 additional simulations with life history parameters set as in reference scenario Sc3, but

with different release settings. In the first simulation, releases were scheduled as in Sc3, but the initial position of larvae was uniformly distributed over a rectangle circumscribing the polygon described by McCleave et al. (1987), as in Kettle & Haines (2006). In the second simulation, the initial position was drawn from a trivariate Gaussian distribution as in Sc3, but releases were uniformly distributed throughout the year (as in Kettle & Haines 2006, Bonhommeau et al. 2009a,b). Both simulations showed poorer fitting performances than scenario Sc3 (for detailed results see Supplement 2).

Migration routes

Our simulated migration trajectories are consistent with the body of knowledge derived from both field surveys and simulation exercises (e.g. McCleave et al. 1998, Kettle & Haines 2006, Bonhommeau et al. 2010). Leptocephali leave the Sargasso Sea, carried by the Antilles Current, towards the Florida Current and then into the Gulf Stream that carries them across the Atlantic Ocean. After the Gulf Stream branches, larvae scatter over the several meanders of the northeast Atlantic circulation to reach Europe and North Africa. The area from which most successful Lagrangian particles originate (between 25–30° N and 50–65° W, see Fig. 5) fits very well with the spawning area hand-drawn by Schmidt (1923; see his Fig. 4) and with the distribution of the smallest leptocephali collected during the Sargasso Sea Eel Expedition 1979 (Fig. 3 in Schoth & Tesch 1982). Notably, none of the larvae released west of the 70° W meridian successfully reached the arrival line. This is in contrast with previous simulation studies (Kettle & Haines 2006, Bonhommeau et al. 2009a,b) that identified the 'best' starting places in the western region (70–75° W) of the Sargasso Sea. However, that region falls outside the supposed reproductive range of the European eel, and is most likely unsuitable for spawning as it is directly influenced by the Antilles Current (Power & McCleave 1983).

The latitudinal distribution of arrivals obtained with the reference scenario is similar to those obtained by previous Lagrangian simulations. However, integrating the body growth model into the coupled physical-biological model allowed us not only to compare our results with those of previous simulations or with presence/absence data, but also to verify the agreement between our modelling work and observed body size patterns. Simulated occurrence limits for different body lengths (Fig. 6) agreed with those derived by Schmidt (1923; his Fig. 4). Note that our figure was obtained by letting Lagrangian particles move over the whole time frame of the simulations (4 yr), without removing them as soon as they crossed the arrival line (but removing those killed by natural mortality). As body growth was also not stopped, a few larvae attained unrealistically high body lengths (>90 mm).

Unfortunately, none of our simulations could replicate the increasing body length gradient (from south to north) observed in the proximity of European shelves (Bast & Strehlow 1990, McCleave et al. 1998). This gradient may result from the fact that some larvae take advantage of frontal jets in the Sargasso Sea (Miller & McCleave 1994, Munk et al. 2010) or from an active east-northeastwards larval migration (Bast & Strehlow 1990). With regards to the first hypothesis, our circulation model may not be able to provide an accurate description of small-scale circulation structures. However, Blanke et al. (2012) recently suggested that migration routes following the Gulf Stream and the North Atlantic Drift are likely to be shorter than those based on interior connections.

To test whether an oriented, active swimming may play a significant role in determining the body length gradient, we ran 4 additional simulations in which we introduced some speculative navigation mechanisms that might guide larval movement towards prescribed geographic directions. In these simulations, larval propulsion was in fact not oriented in the same direction as the oceanic current, but in a fixed direction (east, east-northeast, northeast, north-northeast), with all other settings as in the reference simulation scenario Sc3. See Supplement 2 for detailed results of these simulations. Fig. 8 compares field data (from Bast & Strehlow 1990) with latitudinal body length patterns at the 15° W meridian obtained under scenario Sc3 and the northeast-heading scenario. Although the northeast-heading simulation generated the pattern most similar to field data, none of the simulations were able to replicate it in full. Also, they all showed poorer performances than scenario Sc3 with respect to the 2 indicators d_{median} and d_{iqr}. A further explanation of the observed gradient is that it might reflect a cline in body growth rate from warmer, yet less productive, southern waters to cooler, more productive northern waters. This hypothesis could be tested by incorporating data on primary production into the physical-biological model, and linking body growth to food availability or assuming that larval swimming is oriented towards increasing levels of food availability. Although it would be a very interesting extension of our model, it

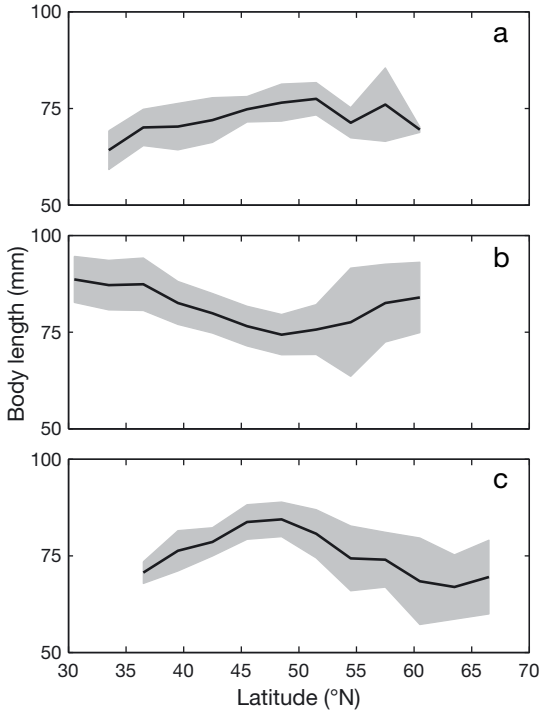

Fig. 8. (a) Latitudinal body size gradients of European eel leptocephali observed near European shelves (from Bast & Strehlow 1990, data referring to the range 11–15° W) compared with those obtained by simulation under reference scenario Sc3 (see Fig. 3), with leptocephali (b) swimming in the direction of the current and (c) heading northeast (all other settings as in the reference scenario; see 'Results: Comparison with experimental data'). Solid lines and shaded areas indicate mean ± SD, respectively

requires a deeper understanding of the physiology, ecology and behaviour of eel larvae and is therefore outside the scope of the present work.

CONCLUSIONS

A fair appraisal of the actual scope of our simulation study requires some caveats. The first regards the spatial and temporal resolution of the ocean model used (1/2°). Higher-resolution (<1/10°) models can provide a description of small-scale structures, such as eddies and filaments, which might contribute to the formation of faster migration pathways (Blanke et al. 2012), perhaps allowing some larvae to carry out their migration faster than suggested by our simulations. However, high-resolution ocean models are currently available only as hindcasts, i.e. they are not based on the assimilation of historical data. In contrast, the ocean reanalyses used in this work are created with the specific purpose of providing a more realistic description of the physical state of the ocean. Obtaining results that are as close as possible to empirical evidence was, in fact, the main goal of our study, and this is the main reason why we decided to use an ocean re-analysis, even if at a slightly coarser scale, rather than using a hindcast at a finer scale. A second caveat is that candidate body growth curves are derived on the basis of a small number of data. In this respect, a comprehensive re-analysis of historical datasets, along with new experimental data, might provide useful information for a more rigorous assessment of body growth. Third, the estimates of survival across the migration derive from the extrapolation of a morphometric relationship referring to the continental phase of the species' life cycle, which might not hold for leptocephali and might therefore impair a precise estimation of the actual mortality rate of leptocephali. However, we could not find any field data on body weight for European eel leptocephali, and using data from aquaculture experiments on other eel species (such as *Anguilla japonica*) might lead to even larger errors. Based on Fig. S1 in Supplement 1 (in which we compare *in situ* data for several anguillid species in different developmental stages) we are convinced that, despite the uncertainty, the potential error is acceptable for the purposes of our work. Finally, the description of eel movement may still be too naive (see 'Discussion: Migration routes') and might be greatly enhanced by a deeper understanding of the behaviour of these larvae.

Despite these limitations, our analysis provides a plausible and consistent interpretation of most existing knowledge about the migration of European eel larvae. Further experimental effort to collect eel larvae at key places and times will help fill the existing knowledge gaps regarding the early life cycle of the European eel. Along with the availability in the near future of eddy-resolving ocean models able to assimilate all the ocean observations and give a more accurate estimate of the high-frequency ocean state, *in situ* estimates of key vital rates are crucial for the development of more realistic models. Integrating oceanographic, demographic and genetic data within coupled physical-biological models (similar to what has been proposed in the multidisciplinary approach of Di Franco et al. 2012) can help decision-makers to develop sustainable management strategies at a global level by identifying critical life history stages and their responses to different environmental forces. In particular, the implementation of a realistic modelling framework of eel migration will provide a valuable tool to investigate possible long-term effects of physical and ecological changes occurring in the ocean on the viability of the European eel.

Acknowledgements. We thank D. Bevacqua, A. J. Crivelli, G. A. De Leo, M. Vichi and 3 anonymous referees for valuable discussion on and advice for this study. Financial support was provided by Politecnico di Milano and the Italian Ministry of Research (PRIN project no. 2006054928 'An Integrated Approach to the Conservation and Management of the European Eel in the Mediterranean Region').

LITERATURE CITED

Als TD, Hansen MM, Maes GE, Castonguay M and others (2011) All roads lead to home: panmixia of European eel in the Sargasso Sea. Mol Ecol 20:1333–1346

Andrello M, Bevacqua D, Maes GE, De Leo GA (2011) An integrated genetic-demographic model to unravel the origin of genetic structure in European eel (*Anguilla anguilla* L.). Evol Appl 4:517–533

Arai T, Otake T, Tsukamoto K (2000) Timing of metamorphosis and larval segregation of the Atlantic eels *Anguilla rostrata* and *A. anguilla*, as revealed by otolith microstructure and microchemistry. Mar Biol 137:39–45

Bast HD, Strehlow B (1990) Length composition and abundance of eel larvae, *Anguilla anguilla* (Anguilliformes: Anguillidae), in the Iberian Basin (northeastern Atlantic) during July–September 1984. Helgol Meersunters 44: 353–361

Bevacqua D, Melià P, Crivelli AJ, De Leo GA, Gatto M (2006) Timing and rate of sexual maturation of European eel in brackish and freshwater environments. J Fish Biol 69(Suppl C):200–208

Bevacqua D, Melià P, Crivelli AJ, De Leo GA, Gatto M (2009) Assessing management plans for the recovery of the European eel: a need for multi-objective analyses. Am Fish Soc Symp 69:637–647

Bevacqua D, Melià P, De Leo GA, Gatto M (2011) Intraspecific scaling of natural mortality in fish: the paradigmatic case of the European eel. Oecologia 165:333–339

Blanke B, Bonhommeau S, Grima N, Drillet Y (2012) Sensitivity of advective transfer times across the North Atlantic Ocean to the temporal and spatial resolution of model velocity data: implication for European eel larval transport. Dyn Atmos Oceans 55–56:22–44

Boëtius J, Harding EF (1985a) A re-examination of Johannes Schmidt's Atlantic eel investigations. Dana 4:129–162

Boëtius J, Harding EF (1985b) List of Atlantic and Mediterranean *Anguilla* leptocephali: Danish material up to 1966. Dana 4:163–249

Bonhommeau S, Chassot E, Rivot E (2008) Fluctuations in European eel (*Anguilla anguilla*) recruitment resulting from environmental changes in the Sargasso Sea. Fish Oceanogr 17:32–44

Bonhommeau S, Blanke B, Tréguier AM, Grima N and others (2009a) How fast can the European eel (*Anguilla anguilla*) larvae cross the Atlantic Ocean? Fish Oceanogr 18:371–385

Bonhommeau S, Le Pape O, Gascuel D, Blanke B and others (2009b) Estimates of the mortality and the duration of the trans-Atlantic migration of European eel *Anguilla anguilla* leptocephali using a particle tracking model. J Fish Biol 74:1891–1914

Bonhommeau S, Castonguay M, Rivot E, Sabatié R, Le Pape O (2010) The duration of migration of Atlantic *Anguilla* larvae. Fish Fish 11:289–306

Brown JH, Gillooly JF, Allen AP, Savage VM, West GB (2004) Toward a metabolic theory of ecology. Ecology 85: 1771–1789

Castonguay M (1987) Growth of American and European eel leptocephali as revealed by otolith microstructure. Can J Zool 65:875–878

Castonguay M, McCleave JD (1987) Vertical distributions, diel and ontogenetic vertical migrations and net avoidance of leptocephali of *Anguilla* and other common species in the Sargasso Sea. J Plankton Res 9:195–214

Cowen RK, Sponaugle S (2009) Larval dispersal and marine population connectivity. Annu Rev Mar Sci 1:443–466

De Leo GA, Gatto M (1995) A size and age-structured model of the European eel (*Anguilla anguilla* L.). Can J Fish Aquat Sci 52:1351–1367

Dekker W (2000) A Procrustean assessment of the European eel stock. ICES J Mar Sci 57:938–947

Desaunay Y, Guérault D (1997) Seasonal and long-term changes in biometrics of eel larvae: a possible relationship between recruitment variation and North Atlantic ecosystem productivity. J Fish Biol 51(Suppl A):317–339

Di Franco A, Coppini G, Pujolar JM, De Leo GA and others (2012) Assessing dispersal patterns of fish propagules from an effective Mediterranean marine protected area. PLoS ONE 7:e52108

Fiksen Ø, Jørgensen C, Kristiansen T, Vikebø F, Huse G (2007) Linking behavioural ecology and oceanography: Larval behaviour determines growth, mortality and dispersal. Mar Ecol Prog Ser 347:195–205

Gallego A, North EW, Petitgas P (2007) Introduction: status and future of modelling physical-biological interactions during the early life of fishes. Mar Ecol Prog Ser 347: 121–126

Halpern BS, Walbridge S, Selkoe KA, Kappel CV and others (2008) A global map of human impact on marine ecosystems. Science 319:948–952

Hannah CG (2007) Future directions in modelling physical–biological interactions. Mar Ecol Prog Ser 347:301–306

Harden Jones FR (1968) Fish migration. Edward Arnold, London

Holyoak M, Casagrandi R, Nathan R, Revilla E, Spiegel O (2008) Trends and missing parts in the study of movement ecology. Proc Natl Acad Sci USA 105:19060–19065

Hoyle SD, Jellyman DJ (2002) Longfin eels need reserves: modelling the effects of commercial harvest on stocks of New Zealand eels. Mar Freshw Res 53:887–895

Kelly JT, Klimley AP (2012) Relating the swimming movements of green sturgeon to the movement of water currents. Environ Biol Fishes 93:151–167

Kettle AJ, Haines K (2006) How does the European eel (*Anguilla anguilla*) retain its population structure during its larval migration across the North Atlantic Ocean? Can J Fish Aquat Sci 63:90–106

Kettle AJ, Vøllestad LA, Wibig J (2011) Where once the eel and the elephant were together: decline of the European eel because of changing hydrology in southwest Europe and northwest Africa? Fish Fish 12:380–411

Kirkpatrick M (1984) Demographic models based on size, not age, for organisms with indeterminate growth. Ecology 65:1874–1884

Kuroki M, Aoyama J, Miller MJ, Wouthuyzen S, Arai T, Tsukamoto K (2006) Contrasting patterns of growth and migration of tropical anguillid leptocephali in the western Pacific and Indonesian Seas. Mar Ecol Prog Ser 309: 233–246

Lecomte-Finiger R (1992) Growth history and age at recruitment of European glass eels *Anguilla anguilla* as revealed by otolith microstructure. Mar Biol 114:205–210

Masina S, Di Pietro P, Navarra A (2004) Interannual-to-decadal variability of the North Atlantic from an ocean

data assimilation system. Clim Dyn 23:531–546
McCleave JD (2008) Contrasts between spawning times of *Anguilla* species estimated from larval sampling at sea and from otolith analysis of recruiting glass eels. Mar Biol 155:249–262
McCleave JD, Kleckner RC (1987) Distribution of leptocephali of the catadromous *Anguilla* species in the western Sargasso Sea in relation to water circulation and migration. Bull Mar Sci 41:789–806
McCleave JD, Kleckner RC, Castonguay M (1987) Reproductive simpatry of American and European eels and implications for migration and taxonomy. Am Fish Soc Symp 1:286–297
McCleave JD, Brickley PJ, O'Brien KM, Kistner DA, Wong MW, Gallagher M, Watson SM (1998) Do leptocephali of the European eel swim to reach continental waters? Status of the question. J Mar Biol Assoc UK 78:285–306
Melià P, Bevacqua D, Crivelli AJ, De Leo GA, Panfili J, Gatto M (2006a) Age and growth of *Anguilla anguilla* in the Camargue lagoons. J Fish Biol 68:876–890
Melià P, Bevacqua D, Crivelli AJ, Panfili J, De Leo GA, Gatto M (2006b) Sex differentiation of the European eel in brackish and freshwater environments: a comparative analysis. J Fish Biol 69:1228–1235
Miller TJ (2007) Contribution of individual-based coupled physical–biological models to understanding recruitment in marine fish populations. Mar Ecol Prog Ser 347: 127–138
Miller MJ, McCleave FD (1994) Species assemblages of leptocephali in the Subtropical Convergence Zone of the Sargasso Sea. J Mar Res 52:743–772
Montgomery JC, Baker CF, Carton AG (1997) The lateral line can mediate rheotaxis in fish. Nature 389:960–963
Munk P, Hansen MM, Maes GE, Nielsen TG and others (2010) Oceanic fronts in the Sargasso Sea control the early life and drift of Atlantic eels. Proc Biol Sci 277: 3593–3599
Nathan R, Wayne MG, Revilla E, Holyoak M, Kadmon R, Saltz D, Smouse PE (2008) A movement ecology paradigm for unifying organismal movement research. Proc Natl Acad Sci USA 105:19052–19059
Oliveira K, Hable E (2010) Artificial maturation, fertilization, and early development of the American eel (*Anguilla rostrata*). Can J Zool 88:1121–1128
Olszewski J, Haehnel M, Taguchi M, Liao JC (2012) Zebrafish larvae exhibit rheotaxis and can escape a continuous suction source using their lateral line. PLoS ONE 7:e36661
Peters RH (1983) The ecological implications of body size. Cambridge University Press, Cambridge
Power JH, McCleave JD (1983) Simulation of the North Atlantic Ocean drift of *Anguilla* leptocephali. Fish Bull 81:483–500
Righton D, Aarestrup K, Jellyman D, Sébert P, van den Thillart G, Tsukamoto K (2012) The *Anguilla* spp. migration problem: 40 million years of evolution and two millennia of speculation. J Fish Biol 81:365–386
Schmidt J (1923) The breeding places of the eels. Philos Trans R Soc Lond B 211:179–208
Schoth M, Tesch FW (1982) Spatial distribution of 0-group eel larvae (*Anguilla* sp.) in the Sargasso Sea. Helgol Meeresunters 35:309–320
Shinoda A, Aoyama J, Miller MJ, Otake T and others (2011) Evaluation of the larval distribution and migration of the Japanese eel in the western North Pacific. Rev Fish Biol Fish 21:591–611
Tanaka H, Kagawa H, Ohta H (2001) Production of leptocephali of Japanese eel (*Anguilla japonica*) in captivity. Aquaculture 201:51–60
Tesch FW (1980) Occurrence of eel *Anguilla anguilla* larvae west of the European continental shelf, 1971–1977. Environ Biol Fishes 5:185–190
Tesch FW (2003) The eel. Blackwell, Oxford
Tsukamoto K, Yamada Y, Okamura A, Kaneko T and others (2009) Positive buoyancy in eel leptocephali: an adaptation for life in the ocean surface layer. Mar Biol 156:835–846
van Ginneken VJT, Maes GE (2005) The European eel (*Anguilla anguilla*, Linnaeus), its lifecycle, evolution and reproduction: a literature review. Rev Fish Biol Fish 15: 367–398
van Ginneken V, Antonissen E, Müller EK, Booms R, Eding E, Verreth J, van den Thillart G (2005) Eel migration to the Sargasso: remarkably high swimming efficiency and low energy costs. J Exp Biol 208:1329–1335
Wang CH, Tzeng WN (2000) The timing of metamorphosis and growth rates of American and European eel leptocephali: a mechanism of larval segregative migration. Fish Res 46:191–205
Wuenschel MJ, Able KW (2008) Swimming ability of eels (*Anguilla rostrata*, *Conger oceanicus*) at estuarine ingress: Contrasting patterns of cross-shelf transport? Mar Biol 154:775–786
Yamada Y, Okamura A, Mikawa N, Utoh T and others (2009) Ontogenetic changes in phototactic behavior during metamorphosis of artificially reared Japanese eel *Anguilla japonica* larvae. Mar Ecol Prog Ser 379:241–251
Zenimoto K, Sasai Y, Sasaki H, Kimura S (2011) Estimation of larval duration in *Anguilla* spp., based on cohort analysis, otolith microstructure, and Lagrangian simulations. Mar Ecol Prog Ser 438:219–228

Editorial responsibility: Alejandro Gallego, Aberdeen, UK

Submitted: November 20, 2012; Accepted: April 9, 2013
Proofs received from author(s): July 4, 2013